

# On-Line Near-Infrared Spectrometer to Monitor Urea Removal in Real Time During Hemodialysis

DAVID S. CHO, JONATHON T. OLESBERG, MICHAEL J. FLANIGAN,\* and MARK A. ARNOLD†

Department of Chemistry and Optical Science and Technology Center (D.S.C., J.T.O., M.A.A.), and Department of Internal Medicine, Cover College of Medicine, (M.J.F.), University of Iowa, Iowa City, Iowa 52242

The *ex vivo* removal of urea during hemodialysis treatments is monitored in real time with a noninvasive near-infrared spectrometer. The spectrometer uses a temperature-controlled acousto optical tunable filter (AOFT) in conjunction with a thermoelectrically cooled extended wavelength InGaAs detector to provide spectra with a  $20\text{ cm}^{-1}$  resolution over the combination region ( $4000\text{--}5000\text{ cm}^{-1}$ ) of the near-infrared spectrum. Spectra are signal averaged over 15 seconds to provide root mean square noise levels of 24 micro-absorbance units for 100% lines generated over the  $4600\text{--}4500\text{ cm}^{-1}$  spectral range. Combination spectra of the spent dialysate stream are collected in real-time as a portion of this stream passes through a sample holder constructed from a 1.1 mm inner diameter tube of Teflon. Real-time spectra are collected during 17 individual dialysis sessions over a period of 10 days. Reference samples were extracted periodically during each session to generate 87 unique samples with corresponding reference concentrations for urea, glucose, lactate, and creatinine. A series of calibration models are generated for urea by using the partial least squares (PLS) algorithm and each model is optimized in terms of number of factors and spectral range. The best calibration model gives a standard error of prediction (SEP) of 0.30 mM based on a random splitting of spectra generated from all 87 reference samples collected across the 17 dialysis sessions. PLS models were also developed by using spectra collected in early sessions to predict urea concentrations from spectra collected in subsequent sessions. SEP values for these prospective models range from 0.37 mM to 0.52 mM. Although higher than when spectra are pooled from all 17 sessions, these prospective SEP values are acceptable for monitoring the hemodialysis process. Selectivity for urea is demonstrated and the selectivity properties of the PLS calibration models are characterized with a pure component selectivity analysis.

Index Headings: Near-infrared spectroscopy; NIR spectroscopy; Urea monitoring; Hemodialysis.

## INTRODUCTION

Current treatment options for people with inadequate renal function are kidney transplantation and dialysis, with the latter being the most prevalent treatment owing to a limited number of available kidneys. The most common form of dialysis delivery is hemodialysis, in which toxic substances are removed from the blood by an *ex vivo* process. Arterial blood is taken from a fistula and passed through a filtration unit where low molecular weight molecules pass through a dialysis membrane into a recipient dialysate solution. Each treatment requires three to four hours to provide sufficient removal of toxins, and treatments are generally performed three times a week.

The extent of dialysis treatment is termed the dialysis dose

and is important for monitoring the efficacy of treatment and the well-being of the person undergoing the dialysis treatment. Dialysis dose is quantified as  $Kt/V$ , where  $K$  is clearance of the dialysis equipment,  $t$  is treatment time, and  $V$  is solute distribution volume. The expression  $Kt/V$  is related to the fraction of the person's urea distribution volume cleared of urea during each treatment.

Despite having a strong influence on the long-term health of dialysis patients,<sup>1–3</sup> the delivered dialysis dose is not routinely monitored.<sup>4,5</sup> The delivered dose depends on a multitude of parameters that influence the efficiency of toxin removal during the dialysis treatment. Accurate measurement of delivered dose requires a detailed assessment of the urea removal dynamics. In practice, the delivered dose is determined from the urea concentration in blood samples collected before and after a dialysis treatment. The inconvenience and costs associated with collecting and analyzing blood samples and the sensitivity of the measurement to the exact timing of the final blood sample makes this process unsuitable for determining optimum dialysis dosage for each treatment. In practice, the dialysis dose is monitored one time per month.

One commonly employed method for estimating dialysis dose is to measure ionic dialysance, which is the average dialysance of ionized substances.<sup>6–9</sup> Ionic dialysance can be measured by using two temperature-corrected conductivity probes placed at the dialyzer inlet and outlet. Since ionic dialysance is strongly correlated to the urea clearance of the dialyzer, ionic dialysance can be used to infer urea clearance. This method is indirect, however, and subject to inaccuracies.

An alternative approach is to measure the concentration of urea in the dialysate, thereby avoiding the complications associated with blood samples. Ideally, the removal of urea from the body can be determined by mass-balance considering the accumulation of urea in the spent dialysate. Successful development of a continuous, *on-line* urea monitor for the dialysate stream could permit quantification of delivered dialysis dose for each patient during each treatment, thereby improving long-term healthcare.

Different sensing methods have been proposed in the literature for measuring urea in dialysate fluid during hemodialysis treatments.<sup>10–15</sup> Most methods are based on urease, which is an enzyme that selectively catalyzes the hydrolysis of urea to produce ammonium and bicarbonate ions. The main drawback of these urease-based approaches is the need to provide active enzyme in the form of a consumable reagent, which increases routine maintenance procedures and adds to the total cost of treatment.

The direct measurement of urea in dialysate fluid by spectroscopic methods represents a reagentless alternative to enzyme-based assays. Mid-infrared spectroscopy has been proposed for such measurements.<sup>16,17</sup> Heise and co-workers

Received 13 June 2007; accepted 28 May 2008.

\* Present address: Marshfield Clinic, 9601 Townline Road, Minocqua, Wisconsin 54548.

† Author to whom correspondence should be sent. E-mail: mark-arnold@uiowa.edu.

have demonstrated the concept by using mid-infrared transmission spectroscopy to measure urea concentrations in plasma dialysate samples collected into a Ringer's buffer.<sup>16</sup> Furthermore, Jensen et al. report the simultaneous measurement of multiple components, including urea, glucose, and phosphate, in dialysate samples.<sup>17</sup>

The NIR method involves transmitting a selected band of NIR radiation through a sample of spent dialysate and extracting the concentration of urea from the resulting spectrum. The feasibility of this approach has been demonstrated with a set of NIR spectra collected from samples obtained during hemodialysis treatments.<sup>18,19</sup> This past work demonstrates the ability to measure urea selectively in the spent dialysis matrix. Standard errors for these urea measurements are 0.3 mM for partial least squares calibration models. In addition, Jensen and co-workers have demonstrated stable urea concentration measurements in the dialysate stream of a hemodialysis unit by using a dual-beam interferometer-based spectrometer.<sup>20</sup>

A Fourier transform near-infrared (FT-IR) spectrometer equipped with a Michelson interferometer was used to collect spectra in the previous work described above. Such FT-IR spectrometers offer many advantages for analytical measurements, including excellent wavelength accuracy and high instrumental signal-to-noise ratios. Nevertheless, interferometer-based spectrometers are not ideal for routine, non-laboratory measurements because these instruments are sensitive to environmental parameters, such as temperature and vibrations, they are expensive to manufacture, and they are difficult to miniaturize.

To advance the development of NIR spectroscopic sensors to monitor and optimize hemodialysis, we have designed a NIR spectrometer based on an acousto-optical tunable filter (AOTF). An AOTF uses pressure waves to create a periodic modulation of the refractive index in a tellurium dioxide crystal. The periodic index modulation forms a diffraction grating. The period of the grating, which determines the wavelength of light diffracted by the crystal, can be tuned by varying the frequency of the pressure wave.<sup>21</sup> The AOTF is an inexpensive, compact, and solid-state device that can be scanned over a wide wavelength range in milliseconds. These features make AOTF technology attractive for NIR spectroscopic sensing in general.<sup>22,23</sup>

Objectives of the work presented here are two-fold. First, performance of the proposed AOTF NIR spectrometer is evaluated for continuous urea measurements in the spent dialysate line of a functioning hemodialysis machine. Second, the robustness of these NIR urea measurements is characterized in terms of accuracy of concentration predictions over time and across patients.

## EXPERIMENTAL

**Instrumentation.** A schematic of the constructed instrument is presented in Fig. 1A. This AOTF spectrometer is similar to other published designs.<sup>24–26</sup> The centerpiece of the spectrometer was the model TEAF5-2.0-2.5-EH/TE-Y AOTF unit purchased from Brimrose Corp. of America (Baltimore, MD). This AOTF unit utilizes a tellurium dioxide crystal designed for measurements in the combination region of the near-infrared spectrum ( $4000\text{--}5000\text{ cm}^{-1}$  or  $2.0\text{--}2.5\text{ }\mu\text{m}$ ) with a spectral resolution of approximately  $20\text{ cm}^{-1}$ . A temperature controller was included to maintain the crystal at a preset temperature of  $30\text{ }^\circ\text{C}$ . The wavelength of the light diffracted by

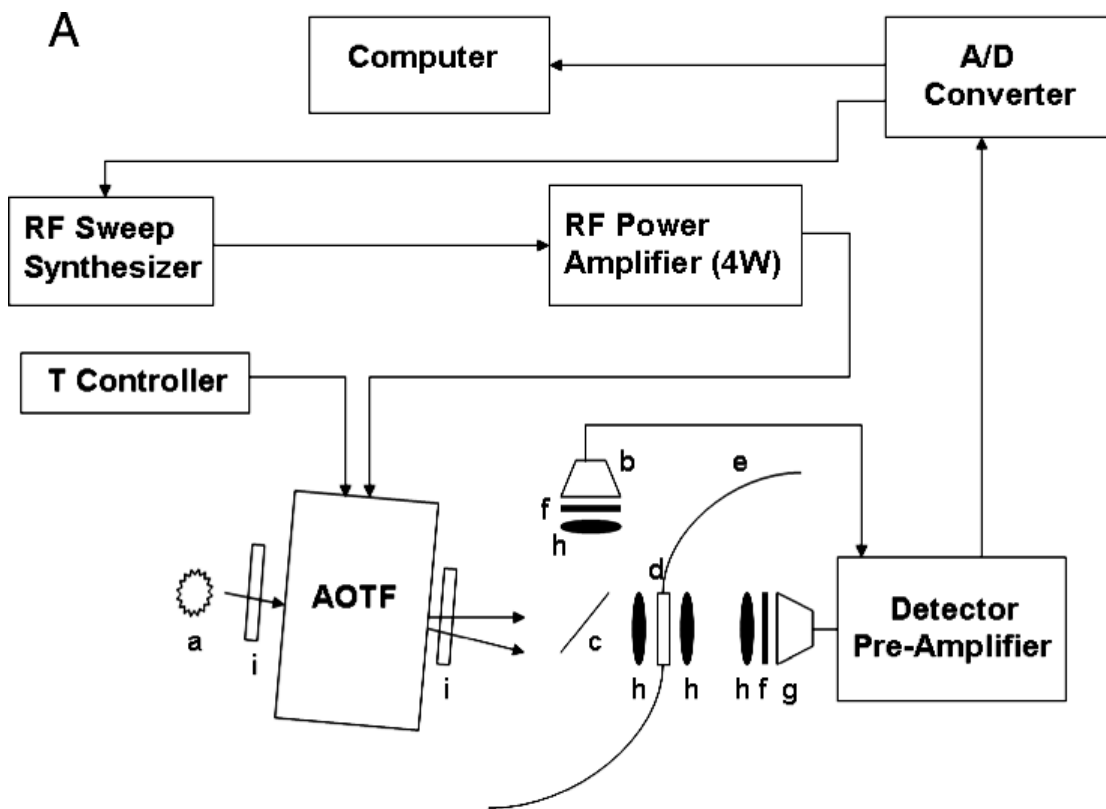
the crystal was determined by an amplified, impedance-matched radio frequency (RF) signal generated from a custom-built RF synthesizer based on an Analog Devices (Norwood, MA) AD9854 direct-digital-synthesis signal generator. The RF output was ramped from 30 to 50 MHz over a period of 10 ms, which provided a full combination spectrum.

A 10-watt, lens-end, tungsten-halogen lamp (Gilway Technical Lamp, Inc., Peabody, MA) provided the incident light, and the diffracted beam was collected at an angle of  $7^\circ$  off normal. A beam splitter was used to reflect 10% of the diffracted light to a reference channel and transmit 90% of this light to a sample channel. The dialysate sample was contained within a tube of thin-wall Teflon with an inner diameter of 1.1 mm. Teflon is an excellent window material for near-infrared spectroscopy and provides a convenient flow-through cell for the measurement.<sup>27,28</sup> Light transmitted through the sample was collected and directed to a two-stage thermoelectrically cooled extended-wavelength InGaAs photodiode detector (Judson Technologies, Montgomeryville, PA). A second detector was used for the reference channel, and a  $1.88\text{ }\mu\text{m}$  long-pass cutoff filter (Barr-Associates, Westford, MA) was positioned before each detector element to restrict signals to the combination region of the near-infrared spectrum. Both the reference and sample channel signals were digitized and recorded with a computer using a model NI-6052E analog-to-digital converter from National Instruments (Austin, TX) in conjunction with the Measurement Studio version 6.0 software.

**Procedures.** Spectral data were collected continuously during dialysis treatments by using a bypass loop in the drain line of the dialyzer. Figure 1B shows the setup schematically. The dialysate passes through a flow-through cell composed of Teflon tubing, where optical measurements are made, a sample draw port, and a thermocouple before returning to the dialysis drain line. A valve positioned in the shunt line parallel to the flow cell restricts flow through the shunt arm and diverts the flow through the optical cell. No active temperature control of the flow-through cell is provided. Measured dialysate temperatures in the measurement loop ranged from  $33$  to  $37\text{ }^\circ\text{C}$ , as determined from the thermocouple probe.

Measurements were performed during 17 separate dialysis sessions of volunteers at the University of Iowa Hospitals and Clinics over the span of ten weeks. In order to determine the actual value of urea concentration in the dialysate, multiple 15 mL dialysate samples were drawn from the measurement loop at evenly spaced intervals during each session. The samples were immediately refrigerated and subsequently analyzed for the concentrations of urea, glucose, lactate, and creatinine. In total, 87 samples were collected for the 17 dialysis sessions, corresponding to an average of 5.1 samples per session. Glucose and lactate concentrations were measured with a YSI Model 2300 Stat Plus analyzer (Yellow Springs Instruments, Yellow Springs, OH). Urea and creatinine concentrations were measured by commercial assays (cat. no. DIUK-01K and DICT-500, respectively; BioAssay Systems, Hayward, CA) using a Lambda 1 UV/Vis spectrometer (Perkin-Elmer, Well-sley, MA).

Near-infrared spectra were collected by focusing the incident light through the Teflon tubing flow-through cell. For 14 of the 17 data collection periods (dialysis sessions), each saved spectrum was the average of 600 sweeps of the AOTF passband collected over 15 seconds. For the remaining three data collection sessions, saved spectra corresponded to the



**B**

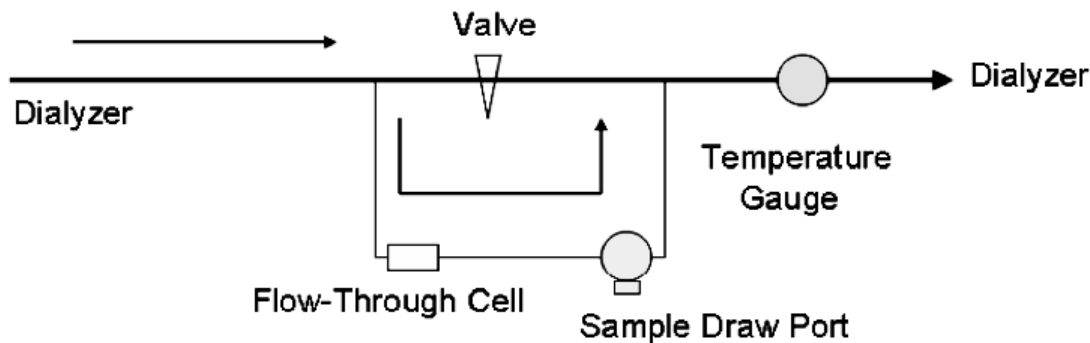


FIG. 1. Schematic diagram of the hardware for *on-line* urea measurements showing (A) the instrument configuration and (B) the flow pattern. Instrumentation block diagram for the AOTF NIR spectrometer includes the (a) light source, (b) reference detector, (c) beam splitter, (d) Teflon sample holder, (e) transfer tubing, (f) 1.88  $\mu\text{m}$  long pass filter, (g) sample detector, (h) lenses, and (i) crossed polarizers. Flow pattern shows relative position of the Teflon tubing that was used as the flow-through cell for collecting spectra (part d in panel A).

average of 400 sweeps collected over 10 seconds. In both cases, multiple spectra were obtained over the one minute period required to draw each dialysate sample. Four and six spectra were saved each minute for the 15 and 10 second collection times, respectively. For sessions with a 15 second spectral averaging time, 71 samples were drawn, which corresponds to 284 spectra ( $71 \times 4$ ). For sessions with a 10 second spectral averaging time, 16 samples were drawn during the collection of 96 spectra ( $16 \times 6$ ). In total, 380 spectra were

collected during the draw of 87 samples over the 17 dialysis sessions. Absorbance spectra were used for all analyses described below, where absorbance spectra were generated as the negative logarithm of the ratio between the corresponding sample and reference channel signals.

## RESULTS AND DISCUSSION

Establishment of the performance characteristics of our AOTF spectrometer is important for comparison to other

spectrometer systems used for NIR sensing.<sup>29</sup> Performance is characterized in terms of the RMS noise of 100% lines. The ability to measure urea is then assessed from an analysis of the resulting *in situ* spectra using the partial least squares (PLS) algorithm.

**Spectrometer Performance.** A critical element for any NIR sensing technology is the signal-to-noise ratio of the instrumentation. The small absorptivities of biomolecules in the combination spectral range generate small absorbance values at clinically relevant concentrations.<sup>30</sup> High instrumental signal-to-noise ratios are required to distinguish these small absorption features relative to the underlying spectral noise.

The signal-to-noise ratio is inversely related to the root mean square (RMS) noise on 100% lines, where a 100% line is generated by dividing a pair of replicate spectra collected from the same sample under the same experimental conditions.<sup>31–33</sup> The signal-to-noise ratio, and correspondingly the RMS noise, varies across the spectral range because of the transmission properties of water.<sup>34</sup>

Across the full spectrum, the minimum RMS noise is 24  $\mu\text{AU}$  obtained over the 4500–4600  $\text{cm}^{-1}$  spectral range with the 15-second averaged spectra. The RMS noise is 27.6  $\mu\text{AU}$  over a wider spectral range (4400–4700  $\text{cm}^{-1}$ ), which contains urea-specific absorption bands. As expected, RMS noise levels are higher for the 10-second averaged spectra compared to the 15-second averaged spectra. The observed relative difference is approximately 1.19, which compares favorably to the theoretical value of 1.22.

Root mean square noise levels are higher compared to previously reported values for our efforts to measure urea by NIR spectroscopy with a Fourier transform (FT) instrument. Spectra from our FT instrument have noise levels on the order of 2  $\mu\text{AU}$ ,<sup>33</sup> which corresponds to a 12-fold improvement compared to the AOTF spectral results. Part of this difference can be accounted for by differences in the acquisition times of 15 seconds for the AOTF spectra and 50 seconds for the FT spectra. The 3.3-fold increase in acquisition time for the FT spectra can explain a 1.8-fold improvement in signal-to-noise and a corresponding reduction in the RMS noise. In addition, a difference in the point spacing for these spectra must be considered. The point spacing was 0.6  $\text{cm}^{-1}$  for the AOTF spectra and 8  $\text{cm}^{-1}$  for the FT spectra. This 13-fold increase in point spacing for FT spectra corresponds to a 3.7-fold improvement in signal-to-noise ratio for FT spectra. Combined, integration time and point spacing explain a factor of seven in the difference in RMS noise between FT and AOTF spectra. After these considerations, RMS noise values from the AOTF spectrometer are within a factor of two of those from the previous FT instrument.

Although RMS noise is higher for spectra collected with the AOTF spectrometer, good analytical performance is still anticipated on the basis of previous studies. Eddy et al. systematically varied resolution and spectral noise to determine the impact of these parameters on NIR urea measurements.<sup>35</sup> Sufficient model accuracy and precision were obtained from spectra corresponding to 16  $\text{cm}^{-1}$  resolution and RMS noise levels of 25  $\mu\text{AU}$ .

**Partial Least Squares Calibration Models for Urea Measurements.** As noted above, 87 unique 15 mL samples were collected during 17 dialysis sessions. Reference methods were used to analyze each sample for the concentrations of urea, glucose, lactate, and creatinine. The degree of concen-

tration correlation between these components was determined by linear regression analysis. The corresponding correlation coefficients ( $r^2$  values) are 0.49, 0.00057, and 0.0090 for urea relative to creatinine, lactate, and glucose, respectively; 0.16 and 0.025 for creatinine relative to lactate and glucose, respectively; and 0.29 between glucose and lactate.

The above results indicate that the largest concentration correlation exists between urea and creatinine. Although this degree of correlation is statistically significant, the concentration of creatinine is very low and should not present a problem for building calibration models for urea. Indeed, urea concentrations range from 1.73 to 8.96 mM, while the range of creatinine concentrations is 0.04 to 0.36 mM. The highest creatinine concentration is below the limit of detection for most NIR calibration models based on high quality spectra. For this reason, no effective interference is expected from creatinine in the calibration models for urea.

Two different methods are presented below to assess the prediction ability of the PLS calibration models. First, a single PLS calibration model is generated by pooling spectra from all 87 samples and then placing all spectra associated with a set of randomly selected samples into an independent prediction set. In a second experiment, calibration models are assessed by evaluating prospective predictions where calibration and prediction data sets are composed of spectra associated with different dialysis sessions. Spectra from early sessions are used to build calibration models, while spectra collected from subsequent dialysis sessions are used to assess prediction accuracy.

**Partial Least Squares Models by Pooling All Spectral Data.** All 380 spectra collected from 87 samples were pooled and randomly divided according to each sample into calibration (70 samples) and prediction (17 samples) data sets. As described before,<sup>34</sup> the calibration data set was further split into training (48 samples) and monitoring (22 samples) data sets for the purpose of optimizing the spectral range and number of PLS factors. Splitting of the calibration data was repeated three times and the resulting standard error of monitoring (SEM) was used to judge model performance. An F-test at the 95% confidence level was used to assess significance of the SEM values determined as a function of the number of factors used in the models. Overall, the combination of number of factors and spectral range that provided the lowest SEM was deemed optimal. The final calibration model was generated by applying the optimized parameters to the full set of calibration data (recombination of training and monitoring data).

The optimized calibration model for urea uses four factors over a spectral range of 4580–4760  $\text{cm}^{-1}$ , which includes a characteristic urea absorption feature centered at 4650  $\text{cm}^{-1}$ .<sup>19</sup> The other characteristic urea absorption band, which is centered at 4550  $\text{cm}^{-1}$ , overlaps to some extent with absorption bands for lactate, glucose, acetate, and creatinine. The final model provides a standard error of calibration (SEC) of 0.30 mM and a standard error of prediction (SEP) of 0.27 mM. The corresponding concentration correlation plot is presented in Fig. 2. Both the calibration and prediction points fall along the ideal unity line with a least squares slope of 0.97 for both calibration and prediction data, 0.92 for the prediction data only, and 0.98 for the calibration data set only. The correlation coefficient is 0.97 for all these data combined.

A plot showing the urea concentration residual as a function

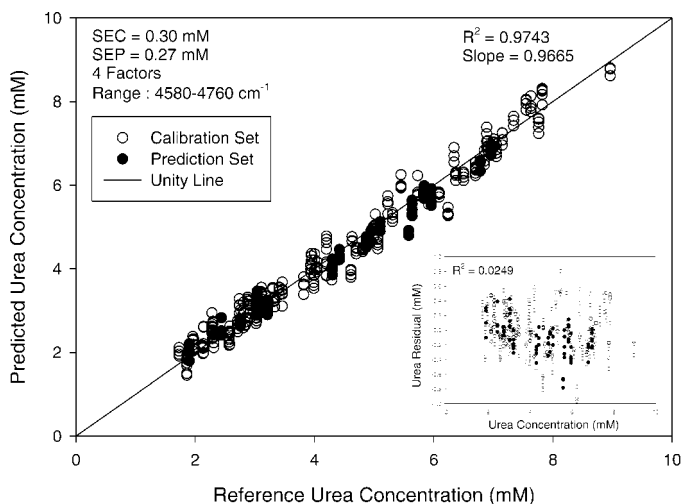


FIG. 2. Concentration correlation plot for urea measurements in flowing dialysate solutions showing calibration (open circles) and prediction (closed circles) points along with the ideal unity (solid line). Inset shows the corresponding residual plot for urea concentration as a function of the concentration of urea in the sample. The solid line in the inset represents the ideal zero response.

of sample urea concentration is provided as an inset in Fig. 2. This residual plot reveals a random relationship between measurement residuals as a function of urea concentration. Similarly, no correlations are evident in residual plots as a function of the concentrations of glucose, creatinine, or lactate. Correlation coefficients are 0.043, 0.0013, 0.081, and 0.026 between the urea concentration residuals and the concentrations of urea, glucose, creatinine, and lactate, respectively.

Selectivity of the model for urea was further evaluated by a pure component selectivity analysis (PCSA).<sup>36</sup> In this analysis, the degree of interference from glucose, creatinine, and lactate was assessed by computing the inner product of the urea PLS regression vector with the pure component aqueous spectrum of each test compound (glucose, creatinine, and lactate). Each pure component aqueous spectrum was collected from a 100 mM solution of the test compound dissolved in water and referenced to a spectrum of water. The resulting inner product of the regression vector and pure component spectra is an estimate of the magnitude of interference created by a 100 mM concentration of the test compound. In practice, the magnitude of this inner product output is divided by the concentration (100 mM) to provide a sensitivity term that relates the magnitude of response for a 1 mM concentration of the test compound. Ideally, the regression vector is orthogonal to the interfering spectral vectors and the inner product is zero.

Results from this PCSA reveal that the inner product values are small, but not zero. Specifically, inner product values are 0.033,  $-0.032$ , and  $-0.26$  mM for lactate, glucose, and creatinine, respectively. The same PCSA calculation for urea results in a value of 1.008. These values indicate that 1 mM concentrations of urea, lactate, glucose, and creatinine would create a model output of 1.008, 0.033,  $-0.032$ , and  $-0.26$  mM, respectively.

The maximum impact of each compound can be estimated by multiplying the selectivity ratio by the highest concentration of that compound in the samples. The highest concentrations are 0.56, 13.1, and 0.36 mM for lactate, glucose, and creatinine, respectively, which correspond to apparent urea

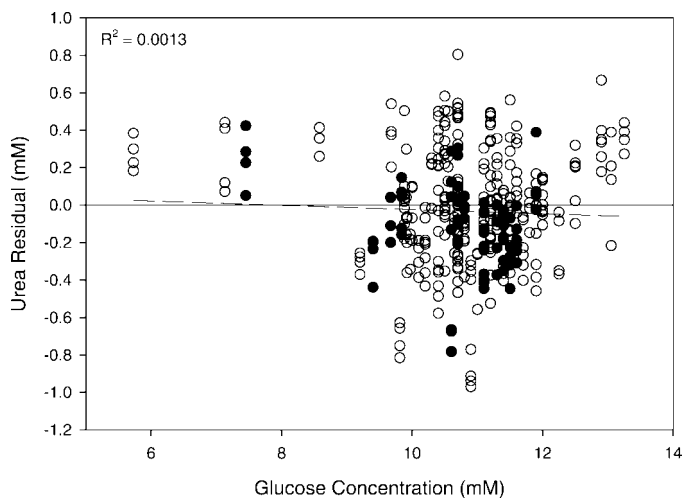


FIG. 3. Residual plot for urea concentrations as a function of the concentration of glucose showing calibration (open circles) and prediction (closed circles) points along with the ideal unity (solid) and regression (broken) lines.

concentrations of  $+0.018$ ,  $-0.42$ , and  $-0.09$  mM, respectively. These apparent urea concentrations for lactate and creatinine are well below the standard error of urea predictions (0.27 mM), which indicates that these compounds have no influence on the urea concentration predictions from the PLS calibration model. For glucose, however, the apparent urea concentration is greater than the SEP, which indicates possible interference from glucose, albeit slight. The observed relationship between the urea concentration residual and the concentration of glucose is presented in Fig. 3. This figure reveals no systematic relationship between errors in the prediction of urea concentration as a function of glucose concentration. The least squares slope for this plot is 0.0013.

**Partial Least Squares Models with Prospective Predictions.** In this experiment, the full set of data was split into calibration and prediction data according to dialysis session. The data were split into six different groupings of calibration and prediction data. The first grouping put spectra from the first fourteen dialysis sessions into the calibration data set and spectra from the subsequent three dialysis sessions in the prediction data set. The second grouping used the first ten sessions for calibration and the subsequent seven sessions for prediction. The third, fourth, fifth, and sixth groupings used calibration data from the first 7, 4, 2, and 1 sessions, respectively, along with the corresponding spectra from the subsequent 10, 13, 15, and 16 sessions, respectively, as the prediction data set. For each grouping, optimized calibration models were generated for urea by the same procedure (training and monitoring subsets) described above.

Table I summarizes the results for all optimized calibration models, including results from the six prospective models and the earlier model where all spectra are pooled. In all cases, the optimized number of factors ranges from 3 to 5 and the optimal spectral range encompasses the principal urea absorption band centered at  $4650\text{ cm}^{-1}$ . The best model performance (lowest SEP) is obtained when all data are pooled and some spectra from each session are included in building the PLS calibration model. Nevertheless, clinically acceptable SEP values are obtained from all prospective models, even in the extreme case where spectra from a single session are used to build a model that predicts urea concentrations in all 16 subsequent sessions.

**TABLE I. Results for PLS calibration models generated with spectra from different dialysis sessions used for calibration purposes.**

Calibration data/ prediction data	SEC (mM)	SEP (mM)	Factors	Optimal range (cm <sup>-1</sup> )
Random splitting	0.30	0.27	4	4600–4740
14/3	0.24	0.37	5	4600–4740
10/7	0.24	0.48	3	4600–4740
7/10	0.24	0.47	3	4590–4750
4/13	0.20	0.49	4	4590–4740
2/15	0.23	0.42	4	4610–4730
1/16	0.14	0.52	4	4580–4790

It is interesting to compare calibration models generated from the extreme models summarized in Table I. In this regard, regression vectors are presented in Fig. 4 for the PLS models generated when all spectra are pooled (solid line) and when only spectra from the first dialysis session are used for calibration purposes. These optimized PLS regression vectors are presented in Fig. 4 along with the absorption spectrum of urea. For the most part, these regression vectors are similar in both shape and magnitude, which indicates that the major chemical information necessary to distinguish urea from the chemical matrix is largely extracted from this first set of spectra. The regression vectors for all other prospective PLS calibration models listed in Table I essentially overlap with the calibration vector generated from a random splitting of the full set of spectral data (solid line in Fig. 4). Furthermore, a comparison of these regression vectors and the absorption spectrum of urea reveals that selectivity is achieved from the 4650 cm<sup>-1</sup> absorption band as opposed to the 4550 cm<sup>-1</sup> band.

Two interesting points are evident from the results summarized in Table I. Firstly, the SEC decreases as the number of sessions included in the calibration data set decreases. This trend is consistent with the fact that fewer session spectra results in less spectral variance in the calibration data and lower SEC values. Accordingly, SEP values generally increase as the number of sessions in the calibration model decreases. Higher SEP values are expected as the additional spectral variance in the prediction data set is not accounted for in the calibration model generated from fewer spectra. Secondly, a prediction accuracy better than 0.5 mM is possible when using a single model for multiple subjects, including the situation where no spectra from a given individual are included in the calibration data. Such a global measurement procedure is critical for the potential general use of this technology.

## CONCLUSION

A solid-state AOTF spectrometer is designed and tested for the ability to follow the removal of urea from blood during the hemodialysis process. The resulting spectrometer provides spectra of sufficient quality for urea measurements with a standard error of prediction of 0.30 mM. As a preliminary test of robustness, urea measurements are demonstrated over a 10 day period in a hospital environment during 17 individual hemodialysis treatments. PLS calibration models for urea provide clinically acceptable performance, even under the circumstances where the calibration model is developed from spectra collected during early sessions and this model is used to predict urea concentrations in subsequent dialysis sessions. These findings are similar to those reported for spectra

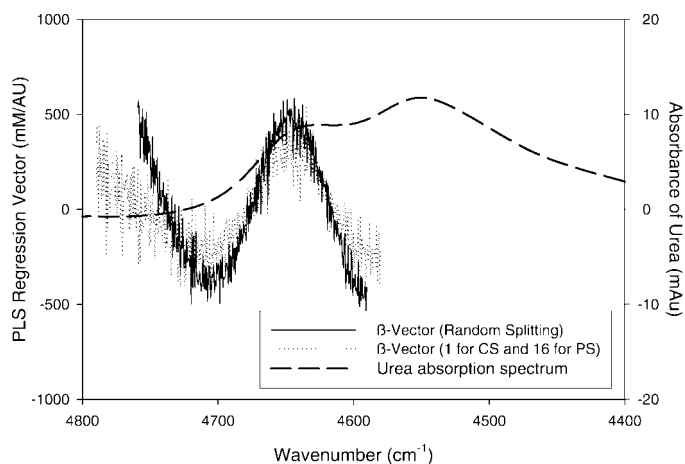


**FIG. 4.** PLS regression vectors ( $\beta$ -vectors) for the measurement of urea based on random splitting of all spectral data (solid line) and based on a 1:16 (calibration-to-prediction) splitting of the individual dialysis session spectra (dotted line). The absorption spectrum of urea is also shown (dashed line).

collected with a more complex dual-beam interferometer-based near-infrared spectrometer.<sup>20</sup> The similarity in shape and magnitude of various regression vectors created from spectra collected during different dialysis sessions suggests that a global calibration model is possible for *on-line* urea measurements.

## ACKNOWLEDGMENTS

This work was supported by grants from the National Institutes of Diabetes and Digestive and Kidney Diseases (DK-02925 and DK-60657). The content of this paper is solely the responsibility of the authors and does not necessarily represent the official views of the National Institute of Diabetes and Digestive and Kidney Diseases or the National Institutes of Health.

- L. A. Szczech, E. G. Lowrie, Z. Li, N. L. Lew, J. M. Lazarus, and W. F. Owen, Jr., *Kidney Int.* **59**, 738 (2001).
- T. F. Parker, L. Husni, W. Huang, N. Lew, and E. G. Lowrie, *Am. J. Kidney Dis.* **23**, 670 (1994).
- R. M. Hakim, J. Breyer, N. Ismail, and G. Schulman, *Am. J. Kidney Dis.* **23**, 661 (1994).
- W. D. Kloppenburg, C. A. Stegeman, M. Hooyssuur, J. Van Der Ven, P. E. De Jong, and R. M. Huisman, *Kidney Int.* **55**, 1961 (1999).
- F. A. Gotch, N. W. Levin, F. K. Port, R. A. Wolfe, and D. E. Uehlinger, *Am. J. Kidney Dis.* **30**, 1 (1997).
- T. A. Depner, T. Greene, F. A. Gotch, J. T. Daugirdas, P. R. Keshaviah, and R. A. Star, *Kidney Int.* **55**, 635 (1999).
- C. D. Manzoni, S. Di Filippo, M. Corti, and F. Locatelli, *Nephrol. Dial. Transplant* **11**, 2023 (1996).
- S. Di Filippo, S. Andrulli, C. Manzoni, and F. Locatelli, *Kidney Int.* **54**, 263 (1998).
- L. Mercadal, T. Petitclerc, M. C. Jaudon, B. Bene, N. Goux, and C. Jacobs, *Arif. Organs* **22**, 1005 (1998).
- F. Locatelli, U. Buoncristiani, B. Canaud, H. Kohler, T. Petitclerc, and P. Zucchelli, *Nephrol. Dial. Transplant* **20**, 22 (2005).
- P. R. Keshaviah, J. P. Ebben, and P. F. Emerson, *Pediatr. Nephrol.* **9**, S2 (1995).
- S. Zamponi, B. L. Cicero, M. Mascini, L. D. Ciana, and S. Sacco, *Talanta* **43**, 1373 (1996).
- P. Jacobs, W. Sansen, and R. Hombrouckx, *Am. Soc. Artif. Int. Org. J.* **40**, M393 (1994).
- B. Canaud, J.-Y. Bosc, M. Leblanc, L. J. Garred, T. Vo, and C. Mion, *Am. J. Kidney Dis.* **31**, 74 (1998).
- M. R. Marshall, P. Santamaria, and J. F. Collins, *Am. J. Kidney Dis.* **31**, 1011 (1998).
- V. R. Konedpati, U. Damm, and H. M. Heise, *Appl. Spectrosc.* **60**, 920 (2006).
- P. S. Jensen, J. Bak, S. Ladefoged, and S. Andersson-Engels, *Spectrochim. Acta, Part A* **60**, 899 (2004).

18. J. T. Olesberg, M. A. Arnold, and M. J. Flanigan, *Clin. Chem.* **50**, 175 (2004).
19. C. V. Eddy and M. A. Arnold, *Clin. Chem.* **47**, 1279 (2001).
20. P. S. Jensen, J. Bak, S. Ladefoged, S. Andersson-Engels, and L. Friis-Hansen, *J. Biomed. Opt.* **9**, 553 (2004).
21. C. D. Tran, *Anal. Chem.* **64**, 971A (1992).
22. L. Bei, G. I. Dennis, H. M. Miller, T. W. Spaine, and J. W. Carnahan, *Prog. Quant. Electron.* **28**, 67 (2004).
23. C. D. Tran, *Anal. Lett.* **33**, 1711 (2000).
24. E. G. Bucher and J. W. Carnahan, *Appl. Spectrosc.* **53**, 603 (1999).
25. C. Pasquini and F. B. Gonzaga, *Anal. Chem.* **77**, 1046 (2005).
26. C. D. Tran, *Talanta* **45**, 237 (1997).
27. G. Legacy and A. Coudreuse, *Eur. Polym. J.* **34**, 1457 (1998).
28. Y. Lee, S. Nah, H. Namkung, and H. Chung, *Appl. Spectrosc.* **59**, 952 (2005).
29. L. Zhang and G. W. Small, *Anal. Chem.* **75**, 5905 (2003).
30. A. K. Amerov, J. Chen, and M. A. Arnold, *Appl. Spectrosc.* **58**, 1195 (2004).
31. D. I. James and R. C. Stanley, *Spectrochemical Analysis* (Prentice Hall, New Jersey, 1988).
32. K. H. Hazen, M. A. Arnold, and G. W. Small, *Anal. Chem.* **70**, 1773 (1998).
33. J. Chen, M. A. Arnold, and G. W. Small, *Anal. Chem.* **76**, 5405 (2004).
34. C. V. Eddy, M. J. Flanigan, and M. A. Arnold, *Appl. Spectrosc.* **57**, 1230 (2003).
35. M. R. Riely, M. Rhiel, X. Zhou, M. A. Arnold, and D. W. Murhammer, *Biotechnol. Bioeng.* **55**, 11 (1995).
36. M. A. Arnold, G. W. Small, D. Xiang, J. Qui, and D. W. Murhammer, *Anal. Chem.* **76**, 2583 (2004).